Supporting Information

Photo-induced Proton-Coupled Electron Transfer Reactions of Acridine Orange: Comprehensive Spectral and Kinetics Analysis

*Thomas T. Eisenhart and Jillian L. Dempsey**

Department of Chemistry, University of North Carolina

Chapel Hill, North Carolina 27599-3290, United States

**email: dempseyj@email.unc.edu*

Index

I. Experimental Methods

General. All solutions for electrochemical or transient absorption analysis were prepared in a nitrogen-filled glovebox. The acetonitrile used (Fisher Sci, HPLC, >99.9%) was degassed with argon and dried with a Pure Process Technology Solvent System. Reagents were purchased from Aldrich, with the exception of TEMPO$^{\bullet}$ (2,2,6,6-Tetramethylpiperidine 1-oxyl, Chem-Impex Intl.). Acridine Orange was purified by dissolving in methanol and precipitating with 0.1 M NaOH before drying *in vacuo* and storing under inert atmosphere. Despite purification, trace amounts of acridinium were still detected in optical spectra. ^{ttb}PhOH was dried *in vacuo* and stored under an inert atmosphere. ^{ttb}PhOD[1] and TEMPOH[2] were prepared according to literature procedures. Tetrabutylammonium hexafluorophosphate was recrystallized from absolute ethanol, dried *in vacuo*, and stored under inert atmosphere. Triethylamine and tetrafluoroboric acid•diethyl ether were degassed via the freeze-pump-thaw method (three cycles) and stored under inert atmosphere.

Transient Absorption Spectroscopy. Transient absorption experiments were performed using a commercially available laser flash photolysis system (Edinburgh Instruments LP920) with laser excitation (532 nm, 5−7 ns fwhm, typically 5.0 ± 0.1 mJ/pulse unless stated otherwise, 5 mm beam diameter, 20 mJ/cm^2) provided by a pulsed Nd:YAG laser (Spectra-Physics Quanta-Ray LAB-170-10)/optical parametric oscillator (VersaScan-MB) combination. To accommodate the pulsed, 1 Hz intensification of the 450 W Xe probe source of the LP920, the laser system was set such that the flash lamps were fired at 10 Hz yet Q-switched at 1 Hz. The timing of the experiment, including laser and probe pulsing, was PC controlled via Edinburgh software (L900). The LP920 was equipped with a multigrating detection monochromator outfitted with a Hamamatsu R928 photomultiplier tube (PMT) in a noncooled housing and a gated charge-coupled device (CCD) (Princeton Instruments, PI-MAX3) such that detection was software selectable. Single-wavelength transient absorption kinetics were monitored with the PMT (10 ns fwhm impulse response function, reliable data out to 400 μs, 300-900 nm) and recorded with a Tektronix TDS-3032C oscilloscope. The gated CCD was used for recording transient spectra covering the entire visible region (400-850 nm, 3 nm spectral bandwidth) at a given time after excitation (10 ns gate width). Data were the result of averaging 40-100 laser shots. Data were collected at room temperature (295 ± 3 K). All samples for transient absorption measurements were prepared in rigorously dry acetonitrile solutions with 100 mM [Bu_4N][PF_6]. Samples were placed into 10 mm path length quartz cuvettes and isolated from atmosphere with a Teflon valve.

Electrochemical Methods. Electrochemistry was performed in a nitrogen filled glovebox with a Pine Instruments WaveNow potentiostat using glassy carbon working electrodes, a platinum counter electrode, and a Ag/$AgNO_3$ (10 mM $AgNO_3$) reference electrode. All scans were performed in acetonitrile solutions with 100 mM [Bu_4N][PF_6] and referenced to the ferrocene/ferrocenium couple ($Fc^{+/0}$). Glassy carbon working electrodes (CH Instruments, 3 mm diameter) were polished with 0.3 micron alumina powder and 0.05 micron alumina powder (CH Instruments, contained no agglomerating agents), rinsed and ultrasonicated for one minute in HPLC grade water to remove residual polishing powder. Spectroelectrochemical measurements were performed with a honeycomb platinum working electrode (Pine Instruments), a platinum counter electrode and a Ag pseudo-reference electrode in a thin-layer quartz cuvette.

II. Additional Figures and Tables

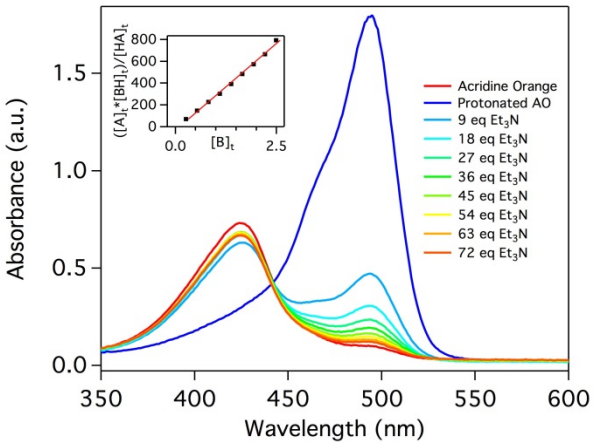

Figure S1. Spectrophotometric titration of acridine orange was used to determine the pK_a in CH_3CN. AO was first completely protonated with 1 equivalent of $HBF_4{\cdot}Et_2O$ before being titrated with additions of triethylamine (pK_a =18.3). An absorbance spectrum was obtained before protonation, after protonation and after every addition of Et_3N. The pK_a of AO (pK_a =19.3) was determined using the method of Saouma *et al.*[3]

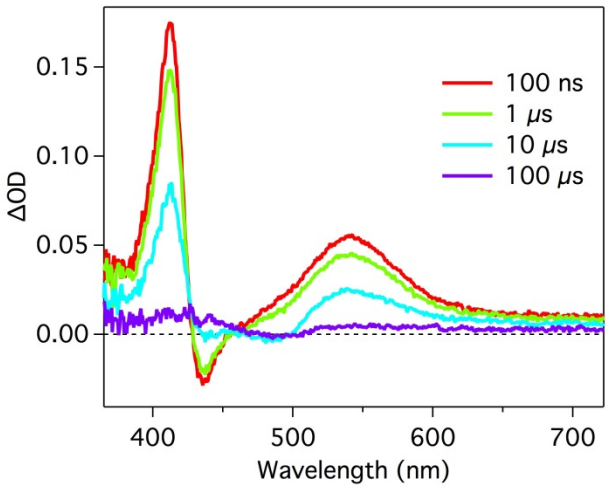

Figure S2. Transient difference spectra of 40 μM AO in CH_3CN at selected time delays after laser excitation. λ_{ex} = 425 nm, 0.1 mM $[Bu_4N][PF_6]$.

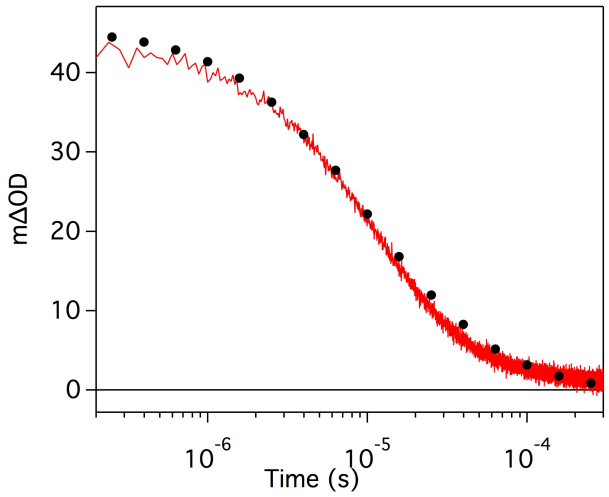

Figure S3. Decay of the triplet excited state of AO monitored at 560 nm in CH_3CN (line) and the corresponding simulated spectrum (markers). Rate constants determined from the simulation and the values previously determined in water at pH 12:[4] k_{nr} (300 s^{-1}, lit: 300 s^{-1}), k_{TT} (5.3×10^9 M^{-1} s^{-1}, lit: 5.5×10^9 M^{-1} s^{-1}), k_S (1.0×10^8 M^{-1} s^{-1}, lit: 3×10^8 M^{-1} s^{-1}). k_{AOH} was determined independently (4.0×10^4 s^{-1}, see Figure S5). 40 μM AO, λ_{ex} = 425 nm, λ_{obs} = 560 nm, 0.1 M $[Bu_4N][PF_6]$.

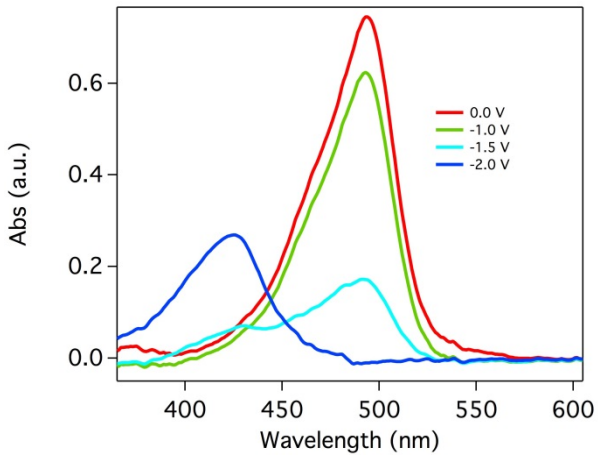

Figure S4. Spectroelectrochemistry of 40 μM AOH^+ in CH_3CN. Optical spectra of AOH^+ were recorded in a spectroelectrochemical cell as applied potentials were stepped to increasingly negative values (hold time = 3 s). Bleaching of the characteristic AOH^+ absorption feature (λ_{max} = 495 nm) is accompanied by growth of a new feature at 425 nm, which we assign to the product of direct reduction, AOH•.[5] A clean isosbestic was not observed, suggesting that AOH^+ is not cleanly converted to the acridinium radical, AOH•. This observation is consistent with the irreversibility observed in CV experiments (Figure S9). Based on the molar extinction coefficient for AOH^+ (ε = 18,000 M^{-1} cm^{-1}), we estimate a lower limit for ε(AOH•) of 6,500 M^{-1} cm^{-1}. Spectra were recorded with a honeycomb platinum working electrode (Pine Instruments), a platinum counter electrode and a Ag pseudo-reference electrode. We were unable to reference the applied potentials directly to ferrocene with this electrochemical cell. As such, these spectra are referenced only to the silver pseudoreference ($Ag^{+/0}$) and the results are qualitative, not quantitative.

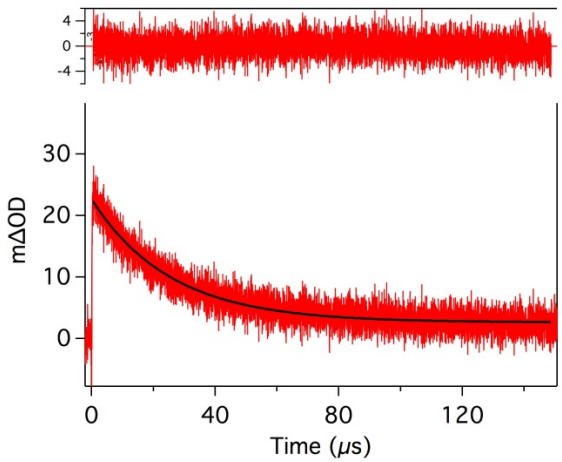

Figure S5. Decay of the triplet excited state of AOH^+ in CH_3CN monitored at 560 nm. Kinetics were fit with a single exponential decay to yield k_{AOH} = 40,000 s^{-1}. 40 μM AOH^+, λ_{ex} = 495 nm, λ_{obs} = 560 nm, 0.1 M [Bu_4N][PF_6].

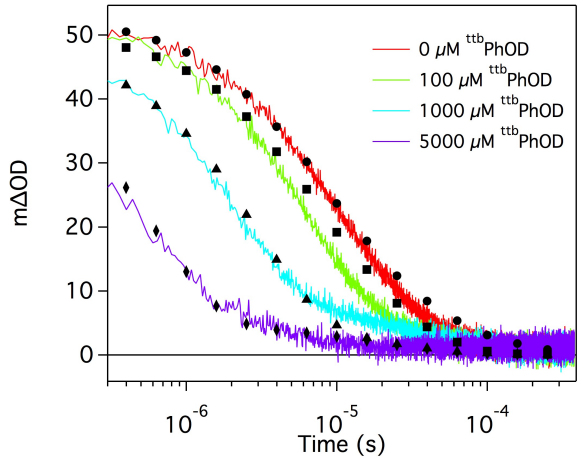

Figure S6. Kinetics traces (lines) of 40 μM AO with 0–1000 μM ^{ttb}PhOD in CH_3CN and the simulated spectra (markers). k_{nr} (300 s^{-1}), k_{TT} (5.3 × 10^9 M^{-1} s^{-1}), k_S (1.0 × 10^8 M^{-1} s^{-1}), k_{CDET} (2.9 × 10^8 M^{-1} s^{-1}), k_{ET} (5.5 × 10^9 M^{-1} s^{-1}), k_{AOH} (4.0 × 10^4 s^{-1}). 40 μM AO, λ_{ex} = 425 nm, λ_{obs} = 560 nm, 0.1 M $[Bu_4N][PF_6]$.

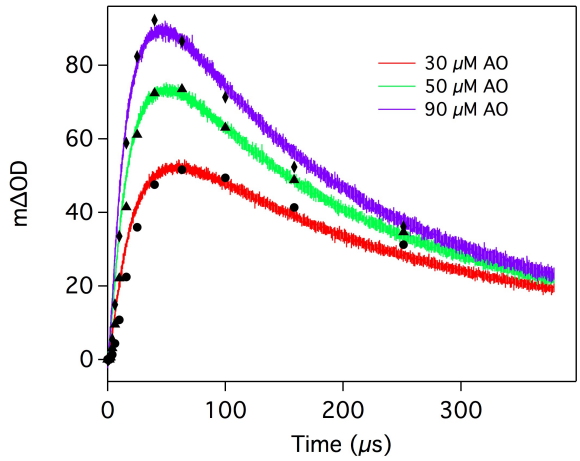

Figure S7. Kinetics traces (lines) of 30–90 μM AO with 500 μM ^{ttb}PhOD in CH_3CN and the simulated spectra (markers). k_{nr} (300 s^{-1}), k_{TT} (5.3 × 10^9 M^{-1} s^{-1}), k_S (1.0 × 10^8 M^{-1} s^{-1}), k_{CDET} (2.9 × 10^8 M^{-1} s^{-1}), k_{ET} (5.5 × 10^9 M^{-1} s^{-1}), k_{PT} (1.0 × 10^9 M^{-1} s^{-1}), k_{AOH} (4.0 × 10^4 s^{-1}, see Figure S5). 40 μM AO, λ_{ex} = 425 nm, λ_{obs} = 460 nm, 0.1 M $[Bu_4N][PF_6]$.

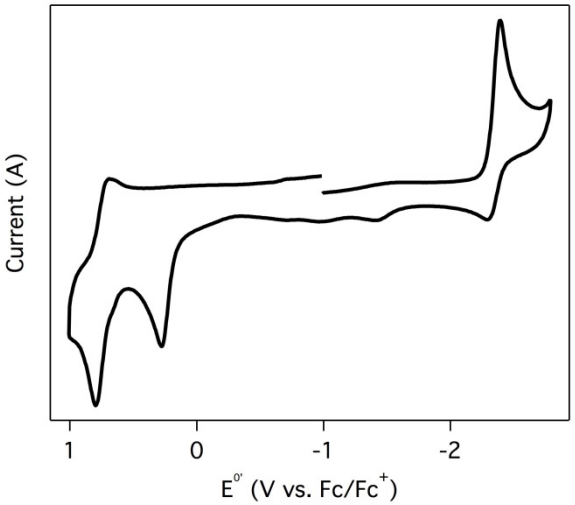

Figure S8. Cyclic voltammogram of 275 μM acridine orange (AO) in CH_3CN with 0.1 M $[Bu_4N][PF_6]$. The irreversible reduction at approximately –2.4 V vs. $Fc^{+/0}$ is attributed to the one-electron reduction of AO ($AO^{0/-}$), followed by reactivity of AO^- on the electrochemical timescale. Scan rate = 500 mV/s.

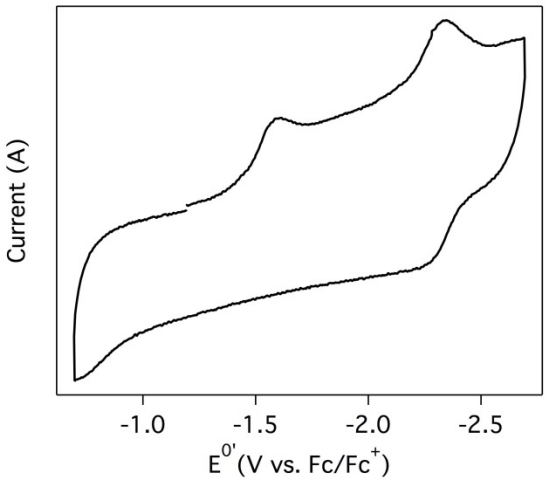

Figure S9. Cyclic voltammogram of 125 μM acridinium orange (AOH^+) in CH_3CN with 0.1 M $[Bu_4N][PF_6]$. The irreversible reduction at approximately –1.6 V vs. $Fc^{+/0}$ is assigned to the $AOH^{+/\bullet}$ couple in agreement with literature values.[6] Scan rate = 500 mV/s.

Table S1. Rate Constants determined from kinetic modeling.

Rate Constant	Value
k_{nr}	$300\ s^{-1}$
k_{TT}	$5.3 \times 10^{9}\ M^{-1}\ s^{-1}$
k_{S}	$1.0 \times 10^{8}\ M^{-1}\ s^{-1}$
k_{CPET}	$3.7 \times 10^{8}\ M^{-1}\ s^{-1}$
k_{CDET}	$2.9 \times 10^{8}\ M^{-1}\ s^{-1}$
k_{ET}	$5.5 \times 10^{9}\ M^{-1}\ s^{-1}$
k_{PT}	$1.0 \times 10^{9}\ M^{-1}\ s^{-1}$
k_{AOH}	$4.0 \times 10^{4}\ s^{-1}$

III. Thermochemical Analysis

Table S2. Reduction potentials in CH_3CN.

Species	$E^{o\prime}$ (V vs. $Fc^{+/0}$)	Reference
$AO^{0/-}$	~ –2.4	This work
$AOH^{+/\bullet}$	~ –1.6	This work
$AO^{3*/-}$	0.18	This work
$AOH^{3*+/\bullet}$	0.53	This work
$^{ttb}PhO^{\bullet/-}$	–0.70	7
$^{ttb}PhOH^{\bullet+/0}$	1.18	7
$TEMPO^{\bullet/-}$	–1.95	7
$TEMPOH^{\bullet+/0}$	0.71	7

Table S3. pK_a values in CH_3CN.

Species	pK_a	Reference
AOH^{+}	19.3	This work
$AOH^{\bullet}$	33.4	This work
$^{ttb}PhOH$	28	7
$^{ttb}PhOH^{\bullet+}$	–3	7
TEMPOH	41	7
$TEMPOH^{\bullet+}$	–4	7

Table S4. S_0–T E_{00} values

Species	E_{00} (eV)	E_{00} (kcal/mol)	Reference
AOH^{+}	2.13	49.2	8
AO	2.58	59.5	This work

E_{00} values for ^{3*}AO and ^{3*}AOH^{+}

The E_{00} ($S_0 \rightarrow T$) for AO has not been measured; but the E_{00} ($S_0 \rightarrow T$) for AOH^+ has been experimentally determined.[8]

$$E_{00}\,(AOH^+ \rightarrow {}^{3*}AOH^+) = +2.13\ \text{eV}$$

From this value, the excited state reduction potential of acridinium triplet can be determined from the equation below.[9,10]

$$E^{\circ\prime}(AOH^{3*+/\bullet}) = E^{\circ\prime}(AOH^{+/\bullet}) + E_{00}(AOH^+) = +0.53\ \text{V vs. } Fc^{+/0}$$

By evaluating the electron transfer quenching of the triplet excited states of AO and AOH^+, Volgelmann has estimated the difference in reduction potentials of ^{3*}AO and $^{3*}AOH^+$.[11]

$$\Delta E^{\circ\prime} = E^{\circ\prime}(AOH^{3*+/\bullet}) - E^{\circ\prime}(AO^{3*/-}) = +0.35\ \text{eV}$$

From this value, the excited state reduction potential of the acridine orange triplet can be estimated. ^{3*}AO is a very weak excited-state oxidant.

$$E^{\circ\prime}(AO^{3*/-}) = +0.18\ \text{V vs. } Fc^{+/0}$$

From this value and the experimentally determined $E^{\circ\prime}(AO^{0/-})$ value , the acridine orange E_{00} ($S_0 \rightarrow T$) value can be estimated with the equation below.

$$E^{\circ\prime}(AO^{3*/-}) = E^{\circ\prime}(AO^{0/-}) + E_{00}$$

$$\underline{E_{00}\,(AO \rightarrow {}^{3*}AO) = +2.58\ \text{eV}}$$

ΔG° for proton transfer reactions[7]

$$\Delta G^{\circ}_{PT} = -RT\ln(K_a) = 2.303RT(pK_a) = (1.37\text{kcal mol}^{-1})pK_a \text{ @ } 298\text{ K}$$

$XH \rightarrow X^- + H^+$	$\Delta G^\circ = (1.37\text{ kcal mol}^{-1})\ pK_a(XH)$
$-(YH \rightarrow Y^- + H^+)$	$\Delta G^\circ = (1.37\text{ kcal mol}^{-1})\ pK_a(YH)$
$XH + Y^- \rightarrow YH + X^-$	$\Delta G^\circ = -(1.37\text{ kcal mol}^{-1})\ [pK_a(YH) - pK_a(XH)]$

ΔG° for electron transfer reactions[7]

$$\Delta G^{\circ}_{ET} = -FE^\circ = -(23.06\text{ kcal mol}^{-1}\text{ V}^{-1})E^\circ$$

$Y + e^- \rightleftharpoons Y^-$	$\Delta G^\circ = -(23.06\text{ kcal mol}^{-1}\text{ V}^{-1})\ E^\circ(Y^{0/-})$
$-(X^+ + e^- \rightleftharpoons X)$	$\Delta G^\circ = -(23.06\text{ kcal mol}^{-1}\text{ V}^{-1})\ E^\circ(X^{+/0})$
$X + Y \rightleftharpoons X^+ + Y^-$	$\Delta G^\circ = -(23.06\text{ kcal mol}^{-1}\text{ V}^{-1})\ [E^\circ(Y^{0/-}) - E^\circ(X^{+/0})]$

ΔG° for CPET reactions were calculated per Hess's Law, as illustrated below.

Calculation of Excited State pK_a for AOH^+

The Förster cycle was utilized to estimate the pK_a of ^{3}*AOH^+ (pK_a*).[12–14]

$$pK_a - pK_a^* = \frac{E_{00}(AOH^+) - E_{00}(AO)}{2.303RT} = \frac{E_{00}(AOH^+) - E_{00}(AO)}{1.37}$$

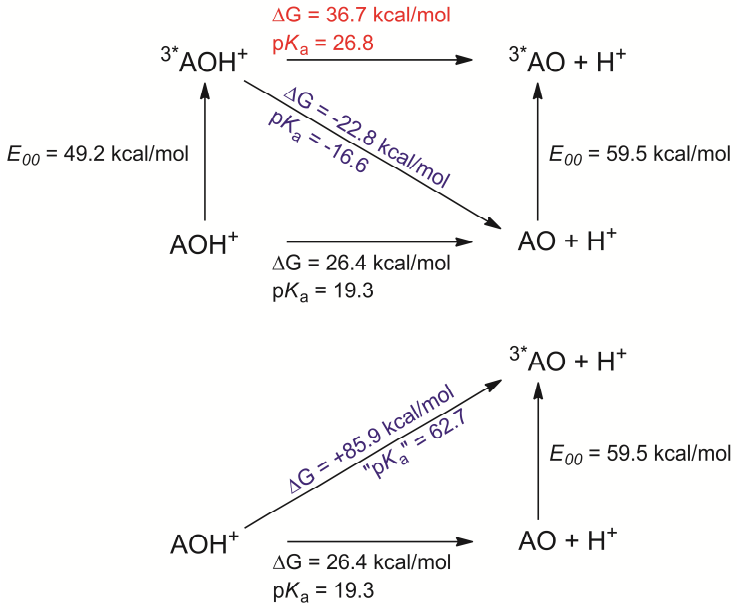

Thermochemical Analysis of Excited State PCET – AO + ^{ttb}PhOH

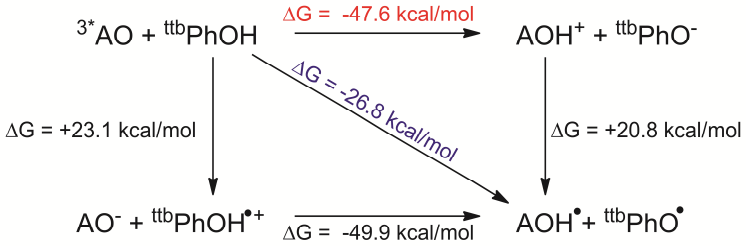

Electron Transfer

$^{3*}AO + {}^{ttb}PhOH \rightarrow AO^{-} + {}^{ttb}PhOH^{\bullet+}$

$\Delta G° = -(23.06 \text{ kcal mol}^{-1} \text{ V}^{-1}) [E°(AO^{3*/-}) - E°({}^{ttb}PhOH^{\bullet+/0})] = +23.1 \text{ kcal mol}^{-1}$

$AOH^{+} + {}^{ttb}PhO^{-} \rightarrow AOH^{\bullet} + {}^{ttb}PhO^{\bullet}$

$\Delta G° = -(23.06 \text{ kcal mol}^{-1} \text{ V}^{-1}) [E°(AOH^{+/\bullet}) - E°({}^{ttb}PhO^{\bullet/-})] = +20.8 \text{ kcal mol}^{-1}$

Proton Transfer

$AO^{-} + {}^{ttb}PhOH^{\bullet+} \rightarrow AOH^{\bullet} + {}^{ttb}PhO^{\bullet}$

$\Delta G° = -(1.37 \text{ kcal mol}^{-1}) [pK_a(AOH^{\bullet}) - pK_a({}^{ttb}PhOH^{\bullet+})] = -49.9 \text{ kcal mol}^{-1}$

See thermal reaction for details

$^{3*}AO + {}^{ttb}PhOH \rightarrow AOH^{+} + {}^{ttb}PhO^{-}$

$\Delta G° = -47.6 \text{ kcal mol}^{-1}$ (per Hess's law, with PT coupled to excited-state deactivation, see below)

Thermochemical Analysis of Excited State PT pathways – AO + ^{ttb}PhOH

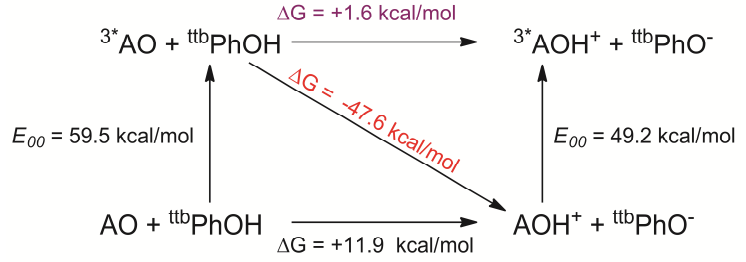

Proton Transfer

$AO + {}^{ttb}PhOH \rightarrow AOH^{+} + {}^{ttb}PhO^{-}$

$\Delta G° = -(1.37 \text{ kcal mol}^{-1}) [pK_a(AOH^{+}) - pK_a({}^{ttb}PhOH)] = +11.9 \text{ kcal mol}^{-1}$

Proton Transfer not coupled to excited state deactivation

$^{3*}AO + {}^{ttb}PhOH \rightarrow {}^{3*}AOH^{+} + {}^{ttb}PhO^{-}$

$\Delta G° = -(1.37 \text{ kcal mol}^{-1}) [pK_a({}^{3*}AOH^{+}) - pK_a({}^{ttb}PhOH)] = +1.6 \text{ kcal mol}^{-1}$

Proton Transfer coupled to excited state deactivation

$^{3*}AO + {}^{ttb}PhOH \rightarrow AOH^{+} + {}^{ttb}PhO^{-}$

$\Delta G° = -47.6 \text{ kcal mol}^{-1}$ (per Hess's Law)

Thermochemical Analysis of Thermal PCET – AO + ^{ttb}PhOH

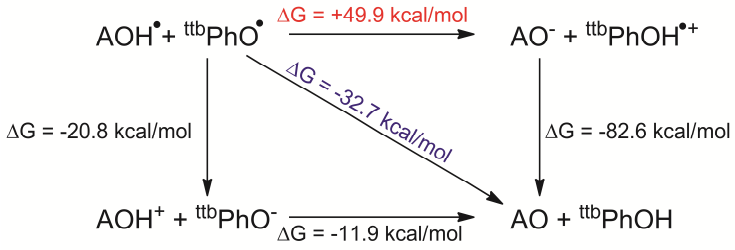

Electron Transfer

$AOH^{\bullet} + {}^{ttb}PhO^{\bullet} \rightarrow AOH^{+} + {}^{ttb}PhO^{-}$

$\Delta G° = -(23.06 \text{ kcal mol}^{-1} \text{ V}^{-1}) [E°({}^{ttb}PhO^{\bullet/-}) - E°(AOH^{+/\bullet})] = -20.8 \text{ kcal mol}^{-1}$

$AO^{-} + {}^{ttb}PhOH^{\bullet+} \rightarrow AO + {}^{ttb}PhOH$

$\Delta G° = -(23.06 \text{ kcal mol}^{-1} \text{ V}^{-1}) [E°({}^{ttb}PhOH^{\bullet+/0}) - E°(AO^{0/-})] = -82.6 \text{ kcal mol}^{-1}$

Proton Transfer

$AOH^{+} + {}^{ttb}PhO^{-} \rightarrow AO + {}^{ttb}PhOH$

$\Delta G° = -(1.37 \text{ kcal mol}^{-1}) [pK_a({}^{ttb}PhOH) - pK_a(AOH^{+})] = -11.9 \text{ kcal mol}^{-1}$

$AOH^{\bullet} + {}^{ttb}PhO^{\bullet} \rightarrow AO^{-} + {}^{ttb}PhOH^{\bullet+}$

$\Delta G° = -(1.37 \text{ kcal mol}^{-1}) [pK_a({}^{ttb}PhOH^{\bullet+}) - pK_a(AOH^{\bullet})] = +49.9 \text{ kcal mol}^{-1}$

$[pK_a({}^{ttb}PhOH^{\bullet+}) - pK_a(AOH^{\bullet})] = -36.4$

$pK_a(AOH^{\bullet}) = +33.4$

Thermochemical Analysis of Excited State PCET – AO + TEMPOH

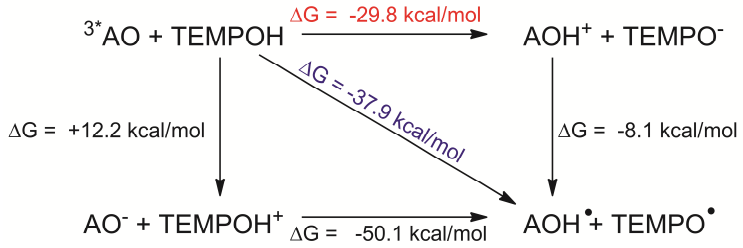

Electron Transfer

$^{3*}AO + TEMPOH \rightarrow AO^{-} + TEMPOH^{\bullet+}$

$\Delta G° = -(23.06\ kcal\ mol^{-1}\ V^{-1})\ [E°(AO^{3*/-}) - E°(TEMPOH^{\bullet+/0})] = +12.2\ kcal\ mol^{-1}$

$AOH^{+} + TEMPO^{-} \rightarrow AOH^{\bullet} + TEMPO^{\bullet}$

$\Delta G° = -(23.06\ kcal\ mol^{-1}\ V^{-1})\ [E°(AOH^{+/\bullet}) - E°(TEMPO^{\bullet/-})] = -8.1\ kcal\ mol^{-1}$

Proton Transfer

$AO^{-} + TEMPOH^{\bullet+} \rightarrow AOH^{\bullet} + TEMPO^{\bullet}$

$\Delta G° = -(1.37\ kcal\ mol^{-1})\ [pK_a(AOH^{\bullet}) - pK_a(TEMPOH^{\bullet+})] = -50.1\ kcal\ mol^{-1}$

See thermal reaction for details

$^{3*}AO + TEMPOH \rightarrow AOH^{+} + TEMPO^{-}$

$\Delta G° = -29.8\ kcal\ mol^{-1}$ (per Hess's law, with PT coupled to excited-state deactivation, see below)

Thermochemical Analysis of Excited State PT pathways – AO + TEMPOH

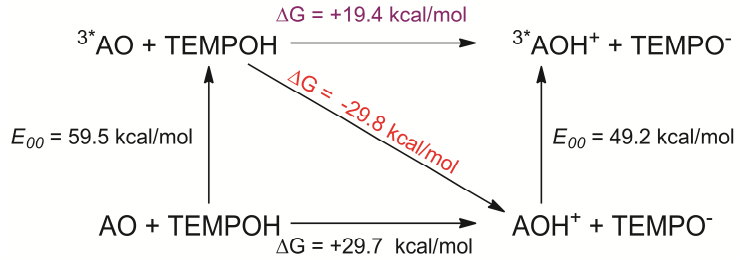

Proton Transfer

$AO + TEMPOH \rightarrow AOH^{+} + TEMPO^{-}$

$\Delta G° = -(1.37\ kcal\ mol^{-1})\ [pK_a(AOH^{+}) - pK_a(TEMPOH)] = +29.7\ kcal\ mol^{-1}$

Proton Transfer not coupled to excited state deactivation

$^{3*}AO + TEMPOH \rightarrow {}^{3*}AOH^{+} + TEMPO^{-}$

$\Delta G° = -(1.37\ kcal\ mol^{-1})\ [pK_a(^{3*}AOH^{+}) - pK_a(TEMPOH)] = +19.4\ kcal\ mol^{-1}$

Proton Transfer coupled to excited state deactivation

$^{3*}AO + TEMPOH \rightarrow AOH^{+} + TEMPO^{-}$

$\Delta G° = -29.8\ kcal\ mol^{-1}$ (per Hess's Law)

Thermochemical Analysis of Thermal PCET – AO + TEMPOH

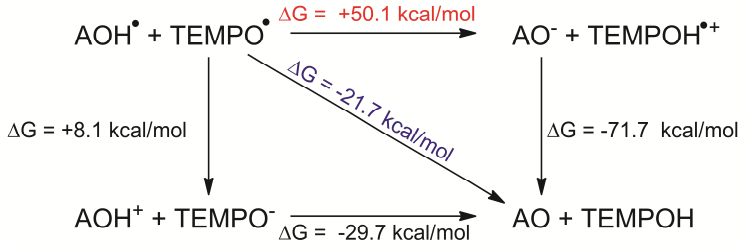

Electron Transfer

$AOH^{\bullet} + TEMPO^{\bullet} \rightarrow AOH^{+} + TEMPO^{-}$

$\Delta G° = -(23.06 \text{ kcal mol}^{-1} \text{ V}^{-1})\,[E°(TEMPO^{\bullet/-}) - E°(AOH^{+/\bullet})] = +8.1 \text{ kcal mol}^{-1}$

$AO^{-} + TEMPOH^{\bullet+} \rightarrow AO + TEMPOH$

$\Delta G° = -(23.06 \text{ kcal mol}^{-1} \text{ V}^{-1})\,[E°(TEMPOH^{\bullet+/0}) - E°(AO^{0/-})] = -71.7 \text{ kcal mol}^{-1}$

Proton Transfer

$AOH^{+} + TEMPO^{-} \rightarrow AO + TEMPOH$

$\Delta G° = -(1.37 \text{ kcal mol}^{-1})\,[pK_a(TEMPOH) - pK_a(AOH^{+})] = -29.7 \text{ kcal mol}^{-1}$

$AOH^{\bullet} + TEMPO^{\bullet} \rightarrow AO^{-} + TEMPOH^{\bullet+}$

$\Delta G° = -(1.37 \text{ kcal mol}^{-1})\,[pK_a(TEMPOH^{\bullet+}) - pK_a(AOH^{\bullet})] = +50.1 \text{ kcal mol}^{-1}$

$[pK_a(TEMPOH^{\bullet+}) - pK_a(AOH^{\bullet})] = -36.5$

$pK_a(AOH^{\bullet}) = 32.5$ (33.4 in ^{ttb}PhOH cycle)

IV. Details of Kinetics Modeling

Scheme S1 Detailed kinetics model

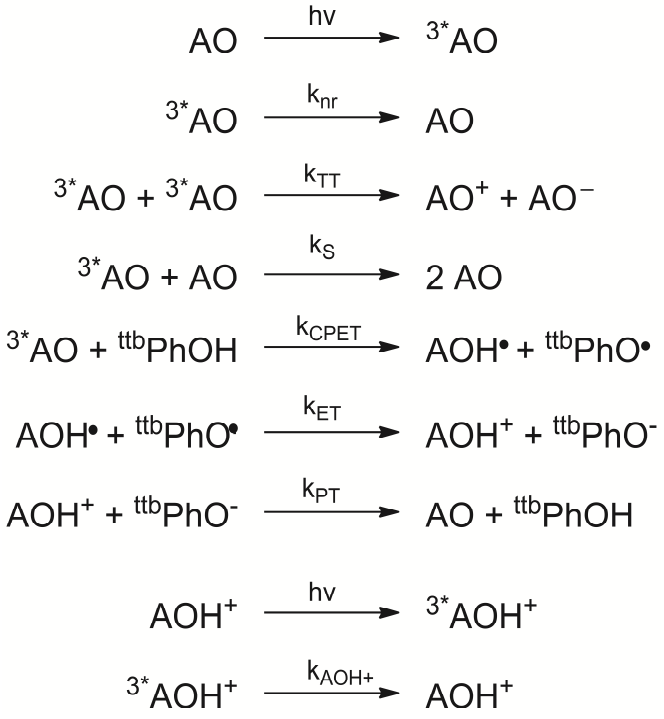

Scheme S2 Differential equations employed for kinetic models

$$\frac{d[^{3*}AO]}{dt} = -k_{nr}[^{3*}AO] - k_{TT}[^{3*}AO]^2 - k_S[^{3*}AO]([AO] - [^{3*}AO]) - k_{CPET}[^{3*}AO][^{ttb}PhOH]$$

$$\frac{d[^{ttb}PhOH]}{dt} = -k_{CPET}[^{3*}AO][^{ttb}PhOH]$$

$$\frac{d[^{ttb}PhO^{\bullet}]}{dt} = k_{CPET}[^{3*}AO][^{ttb}PhOH] - k_{ET}[AOH^{\bullet}][^{ttb}PhO^{\bullet}]$$

$$\frac{d[AOH^{\bullet}]}{dt} = k_{CPET}[^{3*}AO][^{ttb}PhOH] - k_{ET}[AOH^{\bullet}][^{ttb}PhO^{\bullet}]$$

$$\frac{d[^{3*}AOH^{+}]}{dt} = -k_{AOH+}[^{3*}AOH^{+}]$$

$$\frac{d[AOH^{+}]}{dt} = k_{ET}[AOH^{\bullet}][^{ttb}PhO^{\bullet}] - k_{PT}[AOH^{+}][^{ttb}PhO^{-}]$$ (*included only for 460 nm model*)

$$\frac{d[AO]}{dt} = k_{PT}[AOH^{+}][^{ttb}PhO^{-}]$$ (*included only for 460 nm model*)

To simulate the kinetics traces, this series of differential equations was solved numerically with an ordinary differential equations solver. We utilized ode23 in MATLAB. The details of the simulations and the MATLAB *.m files employed are provided below.

Kinetics at 560 nm

Input needed to complete simulated fits:
Timescale: logtimespan = –8:0.2:–3; timespan = 10.^logtimespan;
Molar extinction coefficients for ^{3*}AO, ^{3*}AOH^{+}, ^{ttb}PhO• (in units of M^{-1} cm^{-1}): eps3AO = 4800; eps3AOH+=3500; epsttbPhO = 250
Vector defining rate constants k_{nr}, k_{TT}, k_{CPET}, k_{ET}, k_S and k_{AOH} in this order: k = [knr; kTT; kCPET; kET; kS; kAOH];
Vector defining initial concentrations of ^{3*}AO, ^{ttb}PhOH, ^{ttb}PhO•, AOH•, ^{3*}AOH^{+}: y0 = [3AO; ttbPhOH; ttbPhOrad; AOHrad; 3AOH+];

TripAO_v4.m (script below) describes the various rate expressions associated with kinetics at a given wavelength, in this case 560 nm. y(x) values represent concentrations, and k(x) values represent rate constants.

```
function [yprime]=TripAO_v4(t,y,k)
%y(1)=3AO, y(2)=ttbPhOH, y(3)=ttbPhOrad, y(4)=AOHrad, y(5)=3AOH+ present due
to trace impurity
%k(1)=knr, k(2)=kTT, k(3)=kCPET, k(4)=kET
%k(5)=kS,k(6)=kAOH;

%decay of 3AO
yprime(1)=-k(1).*y(1)-k(2).*y(1).*y(1)-k(3).*y(1).*y(2)-k(5).*y(1).*(40e-6-
y(1));
%ttbPhOH: loss of ttbPhOH due to CPET quenching of 3AO
yprime(2)=-k(3).*y(1).*y(2);
% ttbPhOradical: formation and loss of ttbPhOradical
yprime(3)=k(3).*y(1).*y(2)-k(4).*y(3).*y(4);
% AOHrad:formation and loss of AOHradical - formed in equal concentration with
ttbPhOradical
yprime(4)=k(3).*y(1).*y(2)-k(4).*y(3).*y(4);
%decay of 3AOH+
yprime(5)=-k(6).*y(5);

yprime=yprime(:);
```

TripAO_Simulated_dOD_v4.m (script below) is used to numerically solve the differential equations provided in TripAO_v4.m based on the initial value inputs. The time-dependent concentration profiles produced for each species are multiplied by the appropriate molar absorptivity coefficients at the wavelength of interest (for species absorbing at 560 nm, see above) and the optical pathlength (defined by the pump probe overlap, 0.5 cm). These absorbance values are summed to yield the simulated transient absorption spectra. The simulated spectra can then be plotted and compared to experimental data.

```
[Tcalc,Ycalc]=ode23s(@(t,y)TripAO_v4(t,y,k),timespan,y0);
%Differential equation solver used to compute a simulated concentration
%profile based on the differential equations describing the electron
%transfer reactions (see TripAO.m)

dOD_calc23_560=Ycalc(:,1)*eps3AO*0.5+Ycalc(:,3)*epsttbPhO*0.5+Ycalc(:,5)*epsAO
H*0.5
```

```
%converts calculated concentration profile into a simulated TA spectrum by
%multiplying the concentration profile by the vector of epsilon values
%dOD_calc23_560 is used for the data at 560 nm.
%Plot Simulated Data
plot(Tcalc,dOD_calc23_560','ko');
```

Kinetics at 460 nm

Input needed to complete simulated fits:
Timescale: logtimespan = –8:0.2:–3; timespan = 10.^logtimespan;
Molar absorptivity coefficients for AOH^+ at 460 nm (in units of M^{-1} cm^{-1}): epsAOH=18100
Vector defining rate constants k_{nr}, k_{TT}, k_{CPET}, k_{ET}, k_S, k_{AOH}, k_{PT} in this order: k = [knr; kTT; kCPET; kET; kS; kAOH; kPT];
Vector defining initial concentrations of $^{3*}AO$, $^{ttb}PhOH$, $^{ttb}PhO•$, AOH•, $^{3*}AOH^+$, $^{ttb}PhO^-$ or AOH^+ (equal conc.), AO and $^{ttb}PhOH$ reformed (equal conc): y0 = [3AO; ttbPhOH; ttbPhOrad; AOHrad; 3AOH+; AOH+; AO];

TripAO_v5.m describes the various rate expressions associated with kinetics at a given wavelength, in this case 460 nm. y(x) values represent concentrations, and k(x) values represent rate constants.

```
function [yprime]=TripAO_v5(t,y,k)
%y(1)=3AO, y(2)=ttbPhOH, y(3)=ttbPhOrad, y(4)=AOHrad, y(5)=3AOH+ present due
to trace impurity, y(6)=ttbPhO- and AOH+ formed in solution, y(7)=AO and
ttbPhOH reformed
%k(1)=knr, k(2)=kTT, k(3)=kCPET, k(4)=kET
%k(5)=kS
%k(6)=kAOH; k(7)=kPT

%decay of 3AO
yprime(1)=-k(1).*y(1)-k(2).*y(1).*y(1)-k(3).*y(1).*y(2)-k(5).*y(1).*(40e-6-
y(1));
%ttbPhOH: loss of ttbPhOH due to CPET quenching of 3AO
yprime(2)=-k(3).*y(1).*y(2);
% ttbPhOradical: formation and loss of ttbPhOradical
yprime(3)=k(3).*y(1).*y(2)-k(4).*y(3).*y(4);
%AOHrad:formation and loss of AOHradical - formed in equal concentration with
ttbPhOradical
yprime(4)=k(3).*y(1).*y(2)-k(4).*y(3).*y(4);
%3AOH+ decay
yprime(5)=-k(6).*y(5);
%Formation and reactivity of AOH+ and ttbPhO- - equal concentrations
yprime(6)=k(4).*y(3).*y(4)-k(7).*y(6).*y(6);
%Recombination of AOH+ and ttbPhO-;
yprime(7)=k(7).*y(6).*y(6);

yprime=yprime(:);
```

TripAO_Simulated_dOD_v5.m (script below) is used to numerically solve the differential equations provided in TripAO_v5.m based on the initial value inputs. The time-dependent concentration profiles produced for each species are multiplied by the appropriate molar absorptivity coefficients at the wavelength of interest (see above) and the optical pathlength (defined by the pump probe overlap, 0.5 cm). These absorbance values are summed to yield the

simulated transient absorption spectra. The simulated spectra can then be plotted and compared to experimental data.

```
[Tcalc,Ycalc]=ode23s(@(t,y)TripAO_v5(t,y,k),timespan,y0);
%Differential equation solver used to compute a simulated concentration
%profile based on the differential equations describing the electron
%transfer reactions (see TripAO.m)

dOD_calc23_460=Ycalc(:,6)*epsAOH*0.5;
%converts calculated concentration profile into a simulated TA spectrum by
%multiplying the concentration profile of AOH+ by the epsilon value
%dOD_calc23_560 is used for the data at 460
plot(Tcalc,dOD_calc23_460','ko');
```

V. References

(1) Miyazaki, S.; Kojima, T.; Mayer, J. M.; Fukuzumi, S. *J. Am. Chem. Soc.* **2009**, *131*, 11615–11624.
(2) Mader, E. A.; Larsen, A. S.; Mayer, J. M. *J. Am. Chem. Soc.* **2004**, *126*, 8066–8067.
(3) Saouma, C. T.; Kaminsky, W.; Mayer, J. M. *J. Am. Chem. Soc.* **2012**, *134*, 7293–7296.
(4) Kellmann, A. *Photochem. Photobiol.* **1971**, *14*, 85–93.
(5) Guha, S. N.; Mittal, J. P. *J. Photochem. Photobiol. A Chem.* **1995**, *2*, 181–188.
(6) Bolton, J. R.; Chan, M. S. *Sol. Energy* **1980**, *24561-574*.
(7) Warren, J. J.; Tronic, T. A.; Mayer, J. M. *Chem. Rev.* **2010**, *110*, 6961–7001.
(8) Chambers, R. W.; Kearns, D. R. *Photochem. Photobiol.* **1969**, *10*, 215–219.
(9) Rehm, D.; Weller, A. *Isr. J. Chem.* **1970**, *8*, 259.
(10) Juris, A.; Balzani, V.; Barigelletti, F.; Campagna, S.; Belser, P.; Von Zelewsky, A. *Coord. Chem. Rev.* **1988**, *84*, 85–277.
(11) Vogelmann, E.; Rauscher, W.; Krameer, H. E. A. *Photochem. Photobiol.* **1979**, *29*, 771–776.
(12) Forster, T. *Z. Elektrochem.* **1950**, *54*, 531–535.
(13) Grabowski, Z. R.; Rubaszewska, W. *J. Chem. Soc. Faraday Trans. 1* **1977**, *73*, 11–28.
(14) Dempsey, J. L.; Winkler, J. R.; Gray, H. B. *J. Am. Chem. Soc.* **2010**, *132*, 16774–16776.